Int. J. Nano Dimens. 2026; 17(1) : 69-75

International Journal of Nano Dimension (IJND)

https://dx.doi.org/10.57647/j.ijnd.2026.1701.04

Original Research

DFT Study of HCl The Clusters Under Nano Confinement of Carbon Fullerenes

Aruna Thaker[1], Arwa Makki[2], Dina Hajar[2], Pradip Sarawade[1,*]

[1]*Advanced Materials Energy Research (AMER), Physics Department, University of Mumbai, Kalina Santacruz, Mumbai, Maharashtra, India*
[2]*Department of Biochemistry, Collage of Science, University of Jeddah, Jeddah, Saudi Arabia*

[*]**Corresponding author:** pradip.sarawade@physics.mu.ac.in

Article History

Received:
16 November 2024

Revised:
22 July 2025

Accepted:
23 July 2025

Published online:
30 July 2025

Published in Issue:
2 January 2026

Abstract:

This report reveals the geometry, vibrational properties, and molecular orbitals with HOMO-LUMO energies of HCl clusters $(HCl)_{n=1-2}$ under the confinement of carbon fullerenes $C_{N=42-52}$ at B3LYP level with basis set 6-311++g(d,p). Due to the effect of the H-bond network, the variation in bond length is observed relative to the variation of diameter of carbon fullerenes from C_{42} to C_{52}. Unexpectedly, the high intermolecular stretching mode (3403.96 cm^{-1}) is observed for a shorter bond length (H-Cl = 1.234 Å) under C_{46}. The confined HCl under C_{52} results in high intensity (57.75 units) for stretching mode 2859.36 cm^{-1} with high polarity prediction but on the other hand confined HCl dimer under C_{44} shows the highest stretching mode in the frequency range 3000 cm^{-1} with compressed bond length (H-Cl = 1.254 Å) which acts as an unsaturated system. For HCl, under the confinement of C_{52}, the bond length increases up to 1.292 Å which is quite greater than the experimental value of free HCl (1.275 Å). Exclusively the band gap energies of both the clusters $(HCl)_{n=1-2}$ are also considered to study H-bond connectivity with carbon atoms by using their (HOMO-LUMO).

Keywords: Carbon fullerenes; DFT; Hydrogen-bond network; Molecular dynamics; Molecular orbitals

Cite this article: Thaker A, Makki A, Hajar D, Sarawade P. DFT Study of HCl The Clusters Under Nano Confinement of Carbon Fullerenes. Int. J. Nano Dimens. 2026;17(1): 69-75. https://doi.org/10.57647/j.ijnd.2026.1701.04

1. Introduction

Carbon fullerene was discovered in 1985 and experimentally produced in different sizes by using high-yielding preparative methods. Fullerenes attract the research area due to their geometry and chemical structure. Also, their derivatives have unique properties, and promising for diverse applications in materials science, pharmaceuticals, and nanotechnology. The recent theoretical studies retain a special place in fullerene science. The structural and electronic characteristics of C_{60} and C_{70} are studied by using DFT within the local density approximation on emerging the intermolecular stretching modes, and the complexity of their physical and chemical behaviour. In some research area, the synthesis, characterization, and biological evaluation of some advanced complexes, highlighting their structural features, chemical reactivity, antimicrobial potency, and potential optoelectronic and therapeutic applications [1, 2]. This study synthesizes and characterizes novel complexes, revealing unique structures, bonding interactions, and potent antimicrobial activities via computational analyses using NBO analysis [3, 4, 5]. Encapsulation of hydrogen molecules in C_{50} fullerene results a few thermodynamically stable and unstable complexes (H_2@C_{50}) [6]. Clusters of hydrogen-bonded molecules are extremely important as model systems in the study of intermolecular interactions and chemical reactivity.

Nowadays, Hydrogen bonding is the most widely investigated class of non-covalent interactions due to its

importance in the chemical and physical properties of molecules as well as its impact on the structures and functions of molecules [7]. In this paper, we study the optimized structure of free and confined HCl monomer in $C_{N=42-52}$ at B3LYP level with basis set 6-311++g(d, p) with semi empirical level AM1. The vibrational analysis of $(HCl)_{n=1-2}$ is observed to be in good agreement with some theoretical studies [8, 9]. Also, the hydrogen bonding in clusters plays an important role in molecular orbital energies and hence for hydrogen chloride it is expected that a change in energy gap and other important parameters, is observed relative to the change in the diameter of carbon fullerenes. For the calculations, the B3LYP density functional method is one of our main theoretical tool, where it belongs to the hybrid approximations for the exchange-correlation functional [10].

2. Computational details

In recent studies, clusters of the various molecules can be studied by using different methods in molecular dynamic (MD) simulations. Free and confined HCl monomer in $C_{N=42-52}$ has been studied at B3LYP level with basis set 6-311++g (d,p). In many studies, Density functional theory (DFT) calculations have been carried out with several hybrid functionals including the Becke three-parameter [11] (B3) with the Perdew and Wang [12] (PW91) and Lee, Yang, and Parr [13] (LYP) correlation functional, standalone functional (HCTH). In this report, the geometries of HCl clusters have been fully optimized with exchange-correlation functional (B3LYP) [14]. Carbon fullerenes with increasing diameter ($C_{N=42-52}$) is optimized by using semi-empirical calculation with the AM1 [15]. Also, the frequency calculations of the optimized structures have been characterized as local minima. These ONIOM (AM1/6-311++g(d,p)) calculations have been carried out with the GAUSSIAN 16 program [16]. All the optimized structures gave no negative vibrational modes showing that all structures were stationary in the geometry optimization procedures. Furthermore, analysis of frontier molecular orbitals has been performed, based on the optimized geometries. The Eigenvalues of HOMO and LUMO and their energy gap reflect the inner activity of the molecule.

3. Results and discussion

3.1 Structural properties

HCl monomer (1.275 Å). The confinement effect on monomer under C_{42} is seen more as its bond length The optimized structures of free and confined HCl clusters under $C_{N=42-52}$ are calculated at the B3LYP level with a semiempirical method with basis set AM1/6-311++g(d,p) shown in Fig. 1. As the B3LYP is a popular functional for its accuracy, optimizing HCl to its precise bond length (1.280 Å) is in quite good agreement with the experimental (H-Cl) is reduced to 1.266 Å which increases bond strength and hence the bond dissociation energy. Conversely, under C_{52} bond length (H-Cl = 1.293 Å) is increased by 0.013 Å with a decrease in bond energy due to low interaction energy between Carbon and HCl monomer.

As shown in Fig. 2, the optimized geometry of free and confined $(HCl)_2$ under $C_{N=42-52}$ presents the confinement effect on the H bond parameters such as bond lengths and bond angles. It is strongly confined under C_{42} with a substantially shorter bond length (H-Cl) and therefore

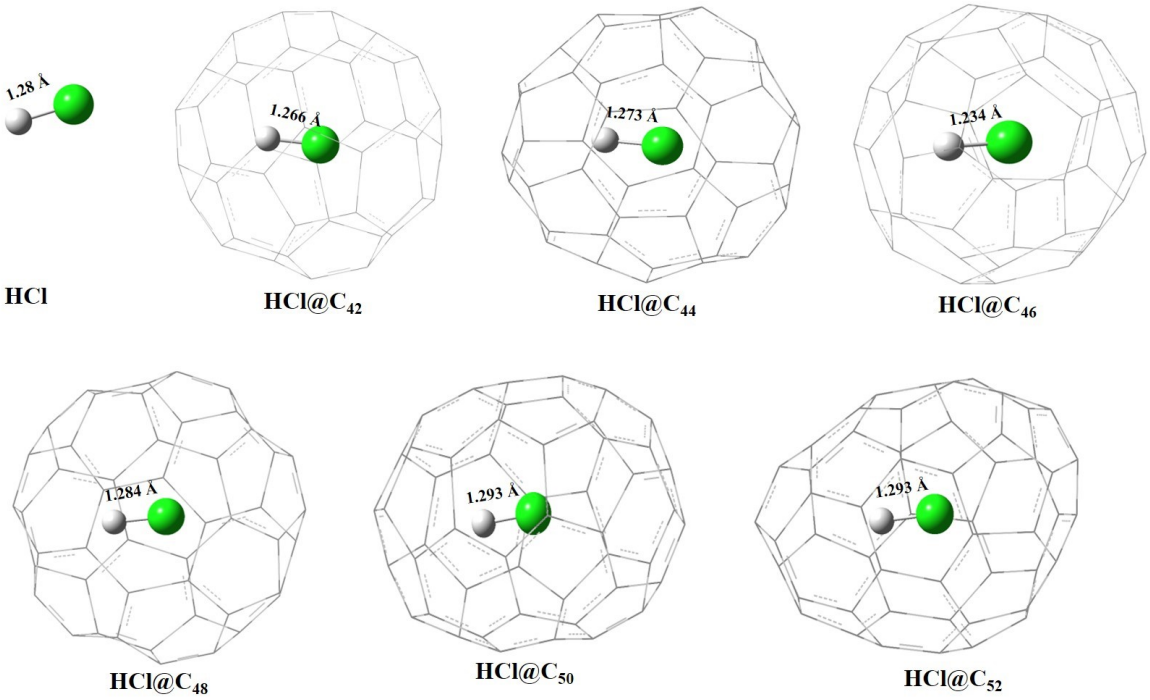

Figure 1. Optimized structures of free and confined HCl under carbon fullerenes $C_{N=42-52}$.

https://dx.doi.org/10.57647/j.ijnd.2026.1701.04

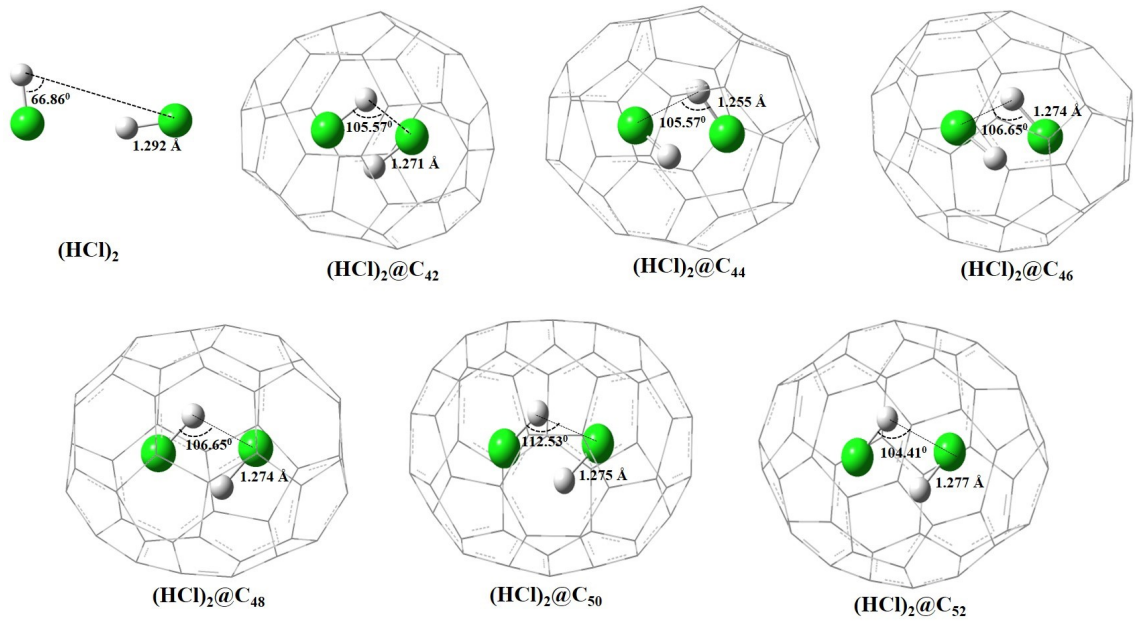

Figure 2. Optimized structures of free and confined $(HCl)_2$ under carbon fullerenes $C_{N=42-52}$.

may be considered as a non-interacting molecule. The increased bond angle (Cl-H-Cl) relative to carbon fullerene size from N=42-50 is due to the increase of repulsion between electron pairs with an increased electronegativity of the central H atom. Interestingly, under C_{52}, the Cl-H-Cl angle is d-ecreased by about 104.414 which contradicts the effect of confinement and causes more repulsion on the bond pairs and as a result, the bond pairs tend to come closer. The intramolecular H-H distance of $(HCl)_2$ has been observed to decrease under the confinement from C_{42} to C_{52}. For non-confined $(HCl)_2$, the H-Cl-H angle indicates the geometry gets affected after confinement due to the number of lone pairs in a molecule leading to a decrease in bond angle. Also, Table 1 indicates that the hydrogen-bond cooperativity increases for all confined $(HCl)_2@C_{N=42-52}$ clusters but seems to reach the limit for free $(HCl)_2$. The average Cl-Cl intramolecular distance for $(HCl)_2$ is reduced by an unequal ratio from N=42-50. For dimer, HCl molecules are oriented approximately parallel with each other due to the reduction in angle H-Cl-H relative to the increased diameter of the carbon fullerenes. Our results strongly suggest that cooperative effects induced by hydrogen bonds are important in HCl. In addition, our results also show that the magnitude of these effects is more important for HCl clusters in combination with different compounds like carbon nanotubes, graphene, H_2O [17], etc.

3.2 Vibrational propertie

Some detailed studies of hydrogen halide clusters are frequently carried out in condensed phases, usually inert gas matrices. Interactions with the matri atoms may influence the vibrational structure of the hydrogen-bonded complex [18]. It is observed that the frequency of free monomer at B3LYP/6-311++g (d,p) level (2927.05

Table 1. Geometrical parameters of free and confined $(HCl)_{n=1-2}$ under carbon fullerenes $C_{N=42-52}$.

Geometrical parameters bond lengths in Å and bond angles in degrees										
System	H-Cl	System	H-Cl		Cl-Cl	H-H	H-Cl-H		Cl-H-Cl	
HCl	1.280	$(HCl)_2$	1.288	1.292	3.890	3.889	25.465	99.430	66.681	168.424
$HCl@C_{42}$	1.266	$(HCl)_2@C_{42}$	1.250	1.271	2.358	1.791	74.763	74.763	105.574	106.754
$HCl@C_{44}$	1.273	$(HCl)_2@C_{44}$	1.255	1.255	2.336	1.827	74.763	72.841	105.574	106.754
$HCl@C_{46}$	1.234	$(HCl)_2@C_{46}$	1.272	1.274	2.500	1.868	72.439	71.976	106.652	107.517
$HCl@C_{48}$	1.284	$(HCl)_2@C_{48}$	1.272	1.274	2.500	1.868	72.439	71.976	106.652	107.517
$HCl@C_{50}$	1.293	$(HCl)_2@C_{50}$	1.275	1.275	2.617	1.794	67.245	67.248	112.526	112.529
$HCl@C_{52}$	1.293	$(HCl)_2@C_{52}$	1.277	1.277	1.882	2.578	67.892	67.893	104.414	104.417

https://dx.doi.org/10.57647/j.ijnd.2026.1701.04

cm^{-1}) is in quite good agreement with the experimental value (2886 cm^{-1}). We define the average frequency shift $|\Delta\nu|$ for each cluster as the difference between the average stretching frequency of $(HCl)_2$ $\langle\nu\rangle$ and the frequency of the monomer (Table 2). Under C_{46}, the high frequency of HCl (3403.96 cm^{-1}) is observed relative to the experimental HCl monomer which affects an increase in the vibrational shift 517.96 cm^{-1}. The stretching frequencies for free HCl and $(HCl)_2$ are higher than experimental values [19]. Confined HCl monomer under C_{52} vibrates with high intensity in frequency range 3140.72 cm^{-1} with high polarity prediction as shown in Table 1. In contrast, HCl confined under C_{46} and $(HCl)_2$ under C_{44} has been observed to decrease its stability, in agreement with the lower intensity of IR bands.

As shown in Fig. 3 (a,b), stretching vibrations of free HCl and $(HCl)_2$ under C_{42} require more energy and show absorption bands in frequency regions 2927.05 cm^{-1} and 2920.69 cm^{-1} respectively which is similar for the alkane functional group. The deviations from the experiment are 41.05 cm^{-1} (HCl) and 50.96 cm^{-1} for $(HCl)_2$. This is possibly related to the neglect of anharmonicity for the isolated species [20]. Our calculations of stretching vibrations for B3LYP are in agreement with the experimental results indicating that hydrogen-bond cooperativity increases for HCl.

3.3 HOMO-LUMO orbitals

The outer orbital energies, known as the HOMO and containing electrons, functions as an electron donor. Consequently, the ionization potential is directly associated with the energy of the HOMO. Conversely, the

Table 2. H-Cl stretching frequencies of free and confined $(HCl)_{n=1-2}$ under $C_{N=42-52}$.

System	Stretching Frequency (ν)	Modes of Vibrations	$^1\langle\nu\rangle$ cm^{-1}	$^2|\Delta\nu|$ cm^{-1}
HCl	2927.05	Stretching	-	41.05
HCl@C_{42}	3173.6	Stretching	-	287.6
HCl@C_{44}	3103.8	Stretching	-	217.8
HCl@C_{46}	3403.96	Stretching	-	517.96
HCl@C_{48}	2960.39	Stretching	-	74.39
HCl@C_{50}	2869.41	Stretching	-	16.59
HCl@C_{52}	2859.36	Stretching	-	26.64
$(HCl)_2$	2860.1, 2915.82	Stretching	2887.96	50.96
$(HCl)_2$@C_{42}	2791.89, 3049.48	Stretching	2920.69	83.69
$(HCl)_2$@C_{44}	3024.02, 3053.64	Stretching	3038.83	201.83
$(HCl)_2$@C_{46}	2962.48, 3044.2	Stretching	3003.34	166.34
$(HCl)_2$@C_{48}	2851.47, 2910.06	Stretching	2880.77	43.77
$(HCl)_2$@C_{50}	2826.97, 2901.86	Stretching	2864.42	27.42
$(HCl)_2$@C_{52}	2887.81, 2916.03	Stretching	2901.92	64.92

$^1\langle\nu\rangle$: Average value of stretching frequencies of $(HCl)_2$

$^2|\Delta\nu|$: Vibrational shift of (HCl) and $(HCl)_2$ relative to its respective experimental values of HCl = 2886 cm^{-1} and $(HCl)_2$ = 2837 cm^{-1} respectively.

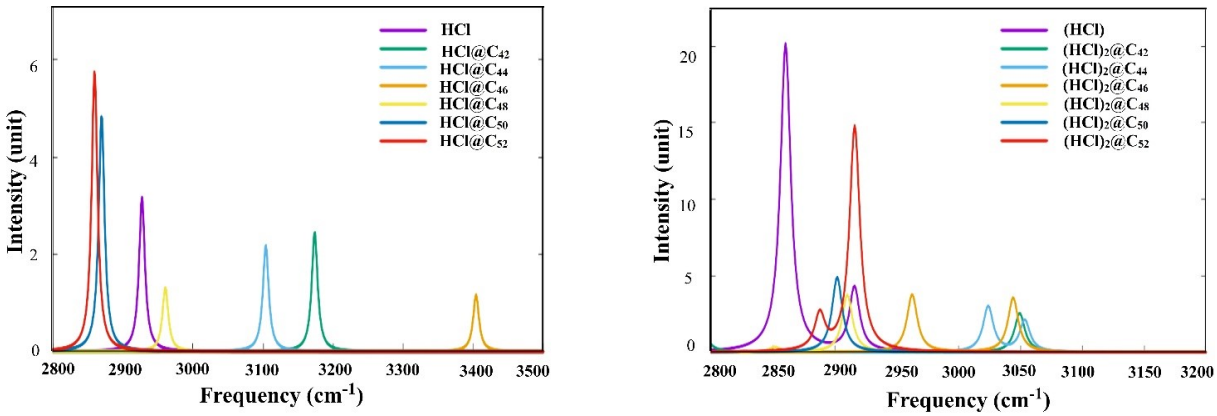

Figure 3. Infra-red Spectra of free and confined (a) $(HCl)_{n=1}$, (b) $(HCl)_{n=2}$ under $C_{N=42-52}$.

https://dx.doi.org/10.57647/j.ijnd.2026.1701.04

LUMO can accept electrons, and its energy level is directly linked to electron affinity [21, 22]. The complex systems with the highest HOMO energy are the HCl@C_{52} (−9.215 eV) and $(HCl)_2$@C_{44} (−7.241 eV). Its elevated energy level allows it as the most effective electron donor. The complex systems that have the lowest LUMO energy are the HCl@C_{52} (−0.795 eV) and free $(HCl)_2$ (−1.136 eV) which signifies that it can be the best electron acceptor. In Fig. 4 (a,b), the complex systems HCl@C_{48} and $(HCl)_2$@C_{50} have the highest energy gap of 8.755 eV and 7.969 eV respectively whereas HCl@C_{52} and $(HCl)_2$@C_{46} with a small frontier orbitals gap of 8.42 eV and 6.547 eV respectively, are more polarisable and associated with a high chemical reactivity and low kinetic stability [23, 24, 25].

Additionally, this lower energy gap allows it to be the softest molecule. The two properties namely enable the computation of essential parameters such as the absolute electron-chemical potential (μ), Global hardness (η), and Global electrophilicity (ω). These three parameters are related to the orbital energies of the HOMO and LUMO (Table 3). It is seen that, the HCl@C_{52} and free $(HCl)_2$ have the lowest values of the ionization potential 9.215 eV and 7.241 eV respectively, so these compounds will be the better electron donors. HCl@C_{52} and free $(HCl)_2$ have the largest value of the affinity 0.795 eV and 1.136 eV, so these are the better electron acceptors. The chemical reactivity varies with the structure of molecules. The chemical hardness (softness) value of HCl@C_{48} (4.210 eV) and $(HCl)_2$@C_{46} (3.274 eV) is lesser (greater) among all the molecules. The value of ω for free $(HCl)_2$ (3.265 eV) indicates that it is a stronger electrophile than all compounds.

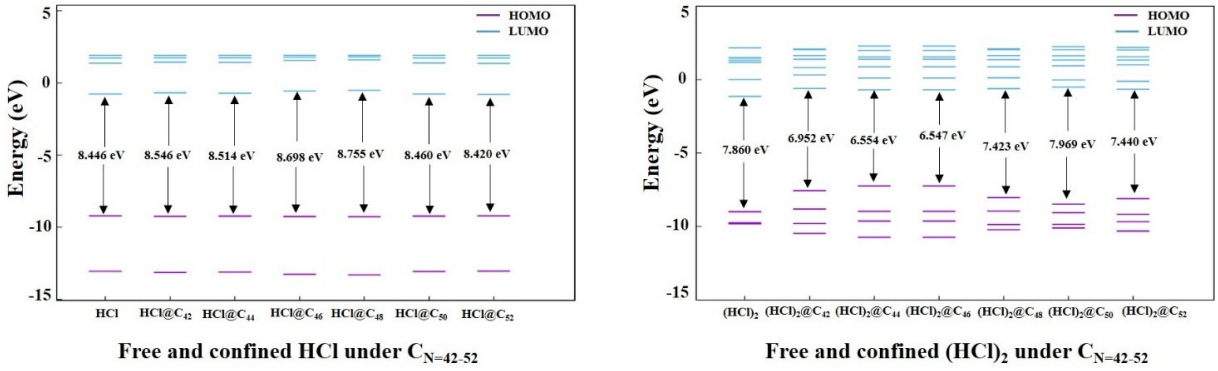

Figure 4. Molecular orbital energy diagram, HOMO-LUMO energy gaps values of free and confined (a) $(HCl)_{n=1}$ (b) $(HCl)_{n=2}$, clusters under $C_{N=42\text{-}52}$.

Table 3. Energy values and global reactivity descriptors of free and confined HCl and $(HCl)_2$ clusters.

System	HOMO	LUMOΔE_g	I	A	η	μ	ω	
HCl	-9.219	-0.773	8.446	9.219	0.773	4.223	-4.996	1.478
HCl@C_{42}	-9.233	-0.687	8.546	9.233	0.687	4.273	-4.960	1.440
HCl@C_{44}	-9.228	-0.715	8.514	9.228	0.715	4.257	-4.971	1.452
HCl@C_{46}	-9.258	-0.559	8.698	9.258	0.559	4.349	-4.908	1.385
HCl@C_{48}	-9.268	-0.513	8.755	9.268	0.513	4.378	-4.890	1.366
HCl@C_{50}	-9.221	-0.761	8.460	9.221	0.761	4.230	-4.991	1.472
HCl@C_{52}	-9.215	-0.795	8.420	9.215	0.795	4.210	-5.005	1.488
$(HCl)_2$	-8.996	-1.136	7.860	8.996	1.136	3.930	-5.066	3.265
$(HCl)_2$@C_{42}	-7.550	-0.598	6.952	7.550	0.598	3.476	-4.074	1.194
$(HCl)_2$@C_{44}	-7.241	0.688	6.554	7.241	0.688	3.277	-3.965	1.199
$(HCl)_2$@C_{46}	-7.388	-0.841	6.547	7.388	0.841	3.274	-4.114	1.293
$(HCl)_2$@C_{48}	-8.030	-0.608	7.423	8.030	0.608	3.711	-4.319	1.257
$(HCl)_2$@C_{50}	-8.476	-0.507	7.969	8.476	0.507	3.984	-4.492	1.266
$(HCl)_2$@C_{52}	-8.094	-0.654	7.440	8.094	0.654	3.720	-4.374	1.286

https://dx.doi.org/10.57647/j.ijnd.2026.1701.04

3.3.1 Microstructure property using TEM

The formation and shape evolution of In_2O_3 nano-assemblies of a better empathetic through TEM studies which were shown in the inset of Fig. 4 (a,b). It can be found that the sample has nearly porous morphology with a diameter and length of nanorod was observed to be 45-50 nm and 70-80 nm respectively.

The diffraction peaks of the highly delicate In_2O_3 nanorods thin film sample S2 exposed inset. It shows marked but uninterrupted ring forms without any additional diffraction marks and rings of subordinate stages, indicating their extremely crystalline assembly.

4. Conclusion

This study presents a detailed quantum chemical investigation of HCl monomers and dimers confined within carbon nanocages (C_{42}-C_{52}) using DFT at the B3LYP level, combined with AM1/6-311++G(d,p) basis sets. The novelty of this work lies in elucidating how confinement within a nanocage environment dramatically alters molecular geometry, electronic distribution, and vibrational characteristics. These confinement-induced structural modifications, such as bond shortening and changes in geometry, directly impact the electronic and vibrational behavior of the system. The small HOMO-LUMO gap of $(HCl)_2@C_{46}$, in particular, highlights its enhanced reactivity, softness, and donor characteristics, making it a valuable model for understanding reactivity trends in host–guest systems. While the current work does not directly involve such complexes, the theoretical framework, particularly the confinement approach and molecular orbital analysis, sets a precedent for extending similar methods to transition metal clusters. Co-based clusters are known for their catalytic and magnetic properties, and exploring their behavior under confinement could open new pathways in nanocatalysis, molecular sensing, and quantum material design. In future work, we aim to apply this confinement strategy to Co complexes to assess how host environments modulate their electronic properties, reactivity, and potential in catalysis or spintronic applications.

Acknowledgments
AT would like to acknowledge the Principal of the M. M. College of Arts, N. M. Institute of Science, H. R. J. College of Commerce, Bhavan's College (Autonomous), Andheri (W), and India. PBS greatly acknowledges the University of Mumbai and DST-SERB for providing financial support through a research grant (EEQ/2020/0002980).

Authors contributions
Authors have contributed equally in preparing and writing the manuscript.

Availability of data and materials
The authors declare that the data supporting the findings of this study are available within the paper.

Conflict of interests
The authors assert that they do not have any identifiable conflicting financial interests or personal relationships that might be perceived to influence the work presented in this paper.

References

1. Majumdar D, Chatterjee A, Feizi-Dehnayebi M, Kiran NS, Tuzun B, and Mishra D. "8-Aminoquinoline derived two Schiff base platforms: Synthesis, characterization, DFT insights, corrosion inhibitor, molecular docking, and pH-dependent antibacterial study." Heliyon 2024; 10. DOI: 10.1016/j.heliyon.2024.e35591
2. Majumdar D, Philip JE, Gassoumi B, Ayachi S, Abdelaziz B, Tüzün B, and Roy S. "Supramolecular clumps of μ2-1, 3-acetate bridges of Cd (II)-Salen complex: Synthesis, spectroscopic characterization, crystal structure, DFT quantization's, and antifungal photodynamic therapy." Heliyon 2024; 10. DOI: 10.1016/j.heliyon.2024.e29856
3. Majumdar D, Frontera A, Roy S, and Sutradhar D. "Experimental and theoretical survey of Intramolecular Spodium Bonds/σ/π-Holes and noncovalent interactions in Trinuclear Zn (II)-Salen type complex with OCN–Ions: a holistic view in Crystal Engineering." ACS omega 2023; 9:1786–97
4. Majumdar D, Roy S, and Frontera A. "The importance of tetrel bonding interactions with carbon in two arrestive iso-structural Cd (ii)–Salen coordination complexes: A comprehensive DFT overview in crystal engineering." RSC advances 2022; 12:35860–72. DOI: 10.1039/d2ra07080d
5. Majumdar D, Dubey A, Tufail A, Sutradhar D, and Roy S. "Synthesis, spectroscopic investigation, molecular docking, ADME/T toxicity predictions, and DFT study of two trendy ortho vanillin-based scaffolds." Heliyon 2023; 9. DOI: 10.1016/j.heliyon.2023.e16057
6. Zeinalinezhad A and Sahnoun R. "Encapsulation of hydrogen molecules in C50 fullerene: an ab initio study of structural, energetic, and electronic properties of H2@ C50 and 2H2@ C50 complexes." ACS Omega 2020; 5:12853–12864. DOI: 10.1021/acsomega.0c00601
7. Hobza P and Havlas Z. "Blue-shifting hydrogen bonds." Chem. Rev. 2000; 100:4253–64. DOI: 10.1021/cr990050q

8. Guedes RC, Couto PC do, and Cabrala BJC. "Binding energy, structure, and vibrational spectra of (HCl) 2–6 and (HF) 2–10 clusters by density functional theory." Journal of Chemical Physics 2003; 118:1272. DOI: 10.1063/1.1528952
9. Huber KP and Herzberg G. Molecular Spectra and Molecular Structure. IV. Constants of Diatomic Molecules, Van Nostrand Reinhold Co. 2013; Springer Science & Business Media. Available from: https://surl.lt/ziovhx
10. Tirado-Rives J and Jorgensen WL. "Performance of B3LYP density functional methods for a large set of organic molecules." J. Chem. Theory and Comput. 2008; 4:297–306. DOI: 10.1021/ct700248k
11. Becke AD. "Density-functional thermochemistry. III. The role of exact exchange. " J. Chem. Phys. 1993; 98:5648. DOI: 10.1063/1.464913
12. Perdew JP and Wang Y. "Accurate and simple analytic representation of the electron-gas correlation energy." Phys. Rev. B 1992; 45:13244. DOI: 10.1103/PhysRevB.45.13244
13. Lee C and Yang W. "Density-functional theory of the electronic structure of molecules". Phys. Rev. B 1995; 37:785. DOI: 10.1146/annurev.pc.46.100195.003413
14. Hamprecht FA, Cohen A, Tozer DJ, and Handy NC. "Development and assessment of new exchange-correlation functionals." J. Chem. Phys. 1998; 109:6264–671. DOI: 10.1063/1.477267
15. Dewar MJS, Zoebisch EG, Healy EF, and Stewart JJ. "AM1: A New General Purpose Quantum Mechanical Molecular Model". J. Am. Chem. Soc. 1985; 115:5348–8. DOI: 10.1021/ja00299a024
16. Gaussian 16, Revision C.01, Frisch MJ, Trucks GW, Schlegel HB, Scuseria GE, Robb MA, Cheeseman JR, Scalmani G, Barone V, Petersson GA, Nakatsuji H, Li X, Caricato M, Marenich AV, Bloino J, Janesko BG, Gomperts R, B. Mennucci HPH, et al. 2016; Gaussian, Inc., Wallingford CT. Available from: https://gaussian.com/g16main/
17. Packert MJ and Clary DC. "Interaction of HCl with water clusters:(H_2O) nHCl, n = 1-3." J. Phys. Chem. 1995; 99:14323–33. DOI: 10.1021/j100039a020
18. Andrews L, Bondybev VE, and English JH. "FTIR spectra of (HF) n species in solid neon." J. Chem. Phys. 1984; 81:3452. DOI: 10.1063/1.448070
19. Andrews L and Bohn RB. "Infrared spectra of isotopic $(HCl)_3$ clusters in solid neon." J. Chem. Phys. 1989; 90:5205. DOI: 10.1063/1.456539
20. Latajka Z and Scheiner S. "Structure, energetics and vibrational spectra of dimers, trimers, and tetramers of HX (X = Cl, Br, I). " Chem. Phys. 1997; 216:37. DOI: 10.1016/S0301-0104(97)00012-8
21. Gece G. "The use of quantum chemical methods in corrosion inhibitor studies. " Corros Sci. 2008; 50:2981–92. DOI: 10.1016/j.corsci.2008.08.043
22. Fukui K. "Role of frontier orbitals in chemical reactions." Science 1982; 218:747–54. DOI: 10.1126/science.218.4574.747
23. Sinha L, Prasad O, Narayan V, and Shukla SR. "Raman, FT-IR spectroscopic analysis and first-order hyperpolarisability of 3-benzoyl-5-chlorouracil by first principles." J Mol Simul. 2011; 37:153–63. DOI: 10.1080/08927022.2010.533273
24. Lewis DFV, Loannides C, and Parke DV. "Interaction of a series of nitriles with the alcohol-inducible isoform of P450: Computer analysis of structure-activity relationships." Xenobiotica 1994; 24:401–8. DOI: 10.3109/00498259409043243
25. Kosar B and Albayrak C. "Spectroscopic investigations and quantum chemical computational study of (E)-4-methoxy-2-[(p-tolylimino) methyl]phenol." Spectrochim Acta. 2011; 78:160–7. DOI: 10.1016/j.saa.2010.09.016